

Soil physical quality of Mollisols quantified by a global index

Pablo Javier Ghiberto^{1*}, Silvia Imhoff^{1,2}, Paulo Leonel Libardi³, Álvaro Pires da Silva⁴, Cassio Antonio Tormena⁵, Miguel Ángel Pilatti¹

¹National University of Litoral/FCA – Dept. of Environmental Science, Kreder 2805 – S3080HOF – Esperanza – Argentina.

²National Council of Scientific and Technical Researches (CONICET), Kreder 2805 – S3080HOF – Esperanza – Argentina.

³University of São Paulo/ESALQ – Dept. of Biosystems Engineering, C.P. 9 – 13418-900 – Piracicaba, SP – Brazil.

⁴University of São Paulo/ESALQ – Dept. of Soil Science.

⁵State University of Maringá – Dept. of Agronomy, Av. Colombo, 5790 – Campus Universitário – 87020900 – Maringá, PR – Brazil.

*Corresponding author <pjghiber@fca.unl.edu.ar>

Edited by: Tairone Paiva Leão

Received February 11, 2014

Accepted August 08, 2014

ABSTRACT: Indicators synthesizing the state of the structural quality and the function of the porous system are useful for assessing soil production capacity as well as the way it may serve natural ecosystems. This research aimed (i) to determine indicators of the state and function of the porous system, (ii) to use them to derive a global index to characterize the soil physical quality, and (iii) to establish a reference pore-size distribution curve for Mollisols from the province of Santa Fe (Argentina). Sixty water retention curves (WRC) of A and B horizons of Mollisols, with clay varying between 119 and 538 g kg⁻¹, organic matter between 5 and 40 g kg⁻¹, and soil bulk density between 1.09 and 1.49 Mg m⁻³, were used. The indicators measured were: pore size distribution, macroporosity (POR_p), air capacity (AC_i) and plant-available water capacity (PAWC) among others. Soils were classified into four groups according to their physical properties and a reference WRC was determined. From this WRC and considering a total porosity of 0.514 m³ m⁻³, POR_p was 0.035 m³ m⁻³, AC_i 0.153 m³ m⁻³, field capacity 0.361 m³ m⁻³, permanent wilting point 0.136 m³ m⁻³ and PAWC 0.225 m³ m⁻³. Both the high silt content and low organic matter content confer on the soil characteristics with low stability, excess of small pores and low porosity of the macropore domain. Consequently, the capacity to quickly drain the water excess and allow root proliferation was not optimal, possibly due to the high silt or clay content and the low sand content, characteristic of the soil matrix of these Mollisols.

Keywords: water release curve, silty-loam, macropore, soil management

Introduction

Soil organic matter, soil structure and the porous system are key attributes of the regulation of water flow, nutrient supply, contaminants adsorption and desorption, and leaching losses as well as gas emissions (Bronick and Lal, 2005; Clothier et al., 2008; Dexter, 2004a). Soil structure conditions influence the pore size distribution that can be described by means of the soil water retention curve (WRC). Pores draining up to the inflection point of the WRC are structural pores whereas the remainder correspond to textural pores, which are conditioned by soil microstructure (Dexter, 2004a). This author suggested using the S index to quantify soil structural quality and demonstrated that it can be used when assessing soil management practices, as it identifies areas of degradation or improvement in the soil physical conditions (Dexter, 2004a,b,c; Dexter and Czyz, 2007).

Other indicators have been suggested by Reynolds et al. (2009) to express either directly or indirectly the state and/or function of porous space: macroporosity, porosity in the matrix domain, air capacity, air capacity in the soil matrix, plant available water capacity, and pore fraction with a diameter, identified either as less or more than 30 µm. By using these indicators they determined an "optimal" pore size distribution, allowing them to study various combinations of soil management practices. Additionally, they characterized pore distribution curves by mode, mean, median, skewness, dispersion and kurtosis. The authors concluded these indicators, together with the S index, are very useful for quantifying

the physical properties of rigid or moderately expansive agricultural soils.

In the Mollisols of Santa Fe, one of the main productive regions in the humid Pampas in Argentina, neither were the above mentioned indicators studied nor a WRC of reference determined, both of which could have been used to distinguish which management techniques promote the improvement or degradation of soil. Due to the importance of establishing these indicators, the aims of this study were: (i) to determine indicators of the state and function of the porous system, (ii) to use them to derive a global index to characterize the soil physical quality, and (iii) to establish a reference pore-size distribution curve for Argiudolls and Hapludolls of the province of Santa Fe, (Argentina).

Materials and Methods

For this study, Argiudolls and Hapludolls representative (INTA, 2014) of those found in the province of Santa Fe (Argentina), with wide variations in texture, organic matter content (OM) and bulk density (ρ_b), were selected (Figure 1, Table 1). For each soil, different soil management conditions were studied so that considerable variability in soil physical properties would be obtained. In each case, disturbed soil samples were collected and used to determine organic carbon by Walkley and Black's method (Jackson, 1982) which were converted to OM by multiplying by 1.724. Particle size and particle density (ρ_p) analyses were carried out by the Bouyoucos hydrometer and pycnometer methods according to Gee and Bauder (1986) and Blake and Hartge (1986a), respectively.

Undisturbed soil samples with stainless steel 100 cm³ cylinders (diameter 5 cm and height 5 cm) were collected at each sampling site to determine the WRCs of

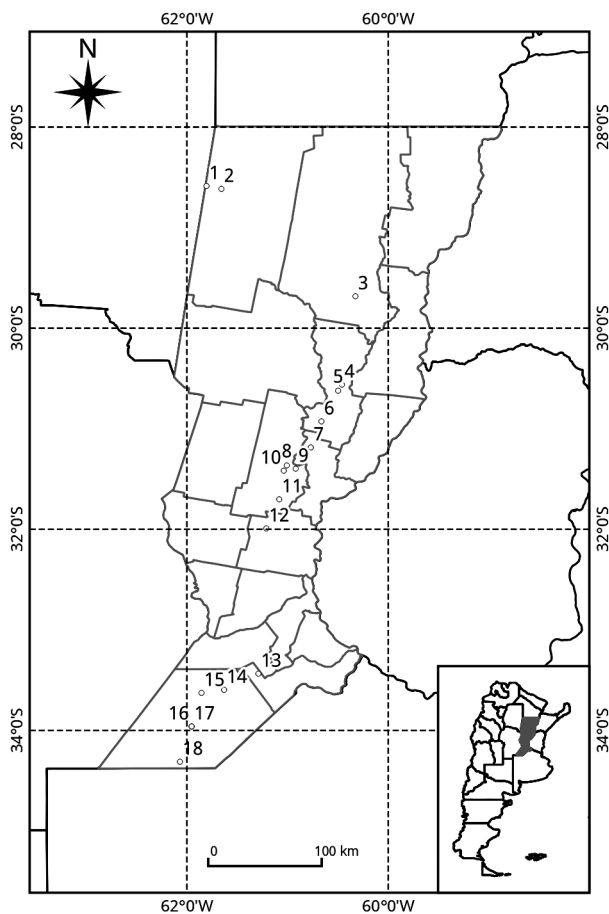


Figure 1 – Soil sampling sites where different soil management conditions were studied. References: 1) Typic Haplustoll, Cuatro Bocas; 2) Typic Argiudoll, Villa Minetti; 3) Aquic Argiudoll, Margarita; 4 and 5) Aquic Argiudoll, Angeloni; 6) Typic Argiudoll, San Justo; 7) Typic Argiudoll, Rincón de Ávila; 8) Aquic Argiudoll, Humboldt; 9) Aquic Argiudoll, Recreo; 10 and 11) Typic Argiudoll, Esperanza; 12) Typic Argiudoll, Loma Alta; 13) Typic Argiudoll, Chabás; 14) Typic Argiudoll, Chovet; 15) Typic Argiudoll, Murphy; 16 and 17) Typic Hapludoll, Santa Isabel; 18) Entic Hapludoll, Saforcada.

A (n = 30) and B (n = 30) horizons. These samples (n = 780) were submitted to the following water potentials: -10, -20, -30, -40, -50, -60, -80, -100 cm of water column in a tension table, and -600, -1,000, -3,000, -6,000 and -15,000 cm of water column in a Richards' pressure chamber (Klute, 1986). Then, the samples were oven-dried and used to determine the ρ_b (Blake and Hartge, 1986b). WRCs that cover at least a range of tension from 10 to 15,000 cm of water column can be used to analyze structural and textural porosity, and consequently the structural condition of the soils (Dexter et al., 2008). This approach was adopted in this study.

Water content data on mass and volume bases were adjusted to equation (1) (van Genuchten, 1980) by using the RETC program Version 6.0 (van Genuchten et al., 2007).

$$\theta_g = \theta_{gr} + (\theta_{gs} - \theta_{gr}) [1 + (\alpha h)^n]^{-m} \quad (1)$$

where: θ_{gs} is the gravimetric saturation water content (kg kg⁻¹); θ_{gr} is the gravimetric residual water content (kg kg⁻¹); α is inversely related to the bubbling pressure, (cm⁻¹), n and m = (1-1/n) are adjustment parameters and h is the absolute value of the matric potential. Then, subscript "v" will be used to indicate volumetric water content and differentiate it from subscript "g" which stands for gravimetric water content.

WRCs, both in their gravimetric and volumetric form, were normalized, by using equation (2).

$$\Theta = \frac{(\theta_g - \theta_{gr})}{(\theta_{gs} - \theta_{gr})} = [1 + (\alpha h)^n]^{-m}; 0 \leq \Theta \leq 1 \quad (2)$$

Θ being the normalized water content, also called the effective saturation.

From these curve indicators suggested by Reynolds et al. (2002), Dexter (2004a) and Reynolds et al. (2009) namely: pore size distribution curve, S index (S_{gi}), macroporosity (POR_p), porosity of the soil matrix domain (POR_m), air capacity (AC_i), air capacity of the soil matrix (AC_m), plant-available water capacity (PAWC), diameter pore fraction less (FC/POR_i) or more (AC_i/POR_i) than 30 μ m were determined.

Table 1 – Content of organic matter (OM), texture and soil bulk density (ρ_b) of the Mollisols studied.

		OM	Sand	Silt	Clay	ρ_b
		g kg ⁻¹				Mg m ⁻³
A horizons	Mean	26 (27.0)	120 (123.6)	577 (21.3)	236 (23.6)	1.33 (4.7)
	Maximum	40	725	766	340	1.46
	Minimum	10	34	156	119	1.09
B horizons	Mean	13 (48.0)	109 (99.0)	509 (13.8)	337 (25.8)	1.41 (2.4)
	Maximum	31	372	634	538	1.49
	Minimum	5	26	389	224	1.35

Values between parentheses are the respective coefficients of variation in percentage. Classification of soil particles according to the United States Department of Agriculture (USDA).

Pore volume distribution curve

The pore-volume distribution curve for each soil was calculated from the first derivative of equation (1) using the volumetric water content, θ_v ($\text{m}^3 \text{m}^{-3}$), versus $\ln(h)$, and plotted against the equivalent pore diameter (d_e), on a \log_{10} scale (Equation 3). The effective pore diameter was described by the equation of capillarity (Libardi, 2005), as shown in equation (4), and was used to describe the pore volume distribution function

$$S_v(h) = -mn(\theta_{vs} - \theta_{vr}) \alpha^n h^n [1 + (\alpha h)^n]^{-(m+1)} \quad (3)$$

$$d_e = \frac{4\gamma \cos \omega}{\rho_w g h} \approx \frac{2980}{h}; \quad h > 0(\text{cm}); \quad d_e(\mu\text{m}); \quad 20^\circ\text{C} \quad (4)$$

where: $S_v(h)$ is the slope of the soil WRC as a function of tension (h); $\gamma = 72.8 \text{ gm s}^{-2}$ the surface tension of water, $\omega \approx 0$ the water-pore contact angle, $\rho_w = 0.998 \text{ g cm}^{-3}$ the water density and $g = 980 \text{ cm s}^{-2}$ the gravitational acceleration.

To make the curves comparable, the normalized pore distribution $S^*(h)$ was obtained by dividing $S_v(h)$ by S_{vi} :

$$S^*(h) = \frac{S_v(h)}{S_{vi}} = \frac{m(\alpha h)^n [1 + m^{-1}]^{-(m+1)}}{[1 + (\alpha h)^n]^{-(m+1)}}; \quad 0 \leq S^*(h) \leq 1 \quad (5)$$

where: S_{vi} is the slope of the tangent at its inflection point which was calculated in the soil WRC, $S_{vi}(h)$, using equation (6):

$$S_{vi}(h) = \left| -n(\theta_{vs} - \theta_{vr}) [1 + (\alpha h)^n]^{-(m+1)} \right| \quad (6)$$

Pore-size frequency curves were compared by using measurements of the central tendency and the spread of the curves (Reynolds et al., 2009). Measurements of the central tendency of each evaluated pore frequency distribution curve were the median (d_{median}) and the mode (d_{mode}) calculated as:

$$d_{\text{median}} = d_{0.5} = \frac{2980\alpha}{(\Theta^{-1/m} - 1)^{1/n}}; \quad \Theta = 0.5 \quad (7)$$

$$d_{\text{mode}} = \frac{2980\alpha}{(\Theta_i^{-1/m} - 1)^{1/n}} = \frac{2980\alpha}{m^{-1/m}} \quad (8)$$

Also the geometric mean (d_{mean}), standard deviation (SD), skewness and kurtosis of the pore frequency distribution curves were studied as presented in equations 9, 10, 11 and 12.

$$d_{\text{mean}} = \exp\left(\frac{\ln d_{0.16} + \ln d_{0.5} + \ln d_{0.84}}{3}\right) \quad (9)$$

$$SD = \exp\left(\frac{\ln d_{0.84} - \ln d_{0.16}}{4} + \frac{\ln d_{0.95} - \ln d_{0.05}}{6.6}\right); \quad 1 \leq SD \leq \infty \quad (10)$$

$$\text{Skewness} = \frac{1}{2} \left[\frac{\ln d_{0.16} + \ln d_{0.84} - 2(\ln d_{0.5})}{(\ln d_{0.84} - \ln d_{0.16})} + \frac{\ln d_{0.05} + \ln d_{0.95} - 2(\ln d_{0.5})}{(\ln d_{0.95} - \ln d_{0.05})} \right]; \quad -1 \leq \text{Skew} \leq 1 \quad (11)$$

$$\text{Kurtosis} = \frac{\ln d_{0.05} - \ln d_{0.95}}{2.44(\ln d_{0.25} - \ln d_{0.75})}; \quad 0.41 \leq \text{Kurtosis} \leq \infty \quad (12)$$

Dexter's S_{gi} index

By using soil WRCs adjusted to the gravimetric water content the S_{gi} index was calculated as suggested by Dexter (2004a). For that purpose equation 6 was used and the soil water potential at the point of inflection of each curve (h_{gi}) was determined as:

$$h_{gi} = \frac{1}{\alpha} \left[\frac{1}{m} \right]^{1/n} \quad (13)$$

Macroporosity and Porosity of the Soil Matrix Domain

Macroporosity (POR_p , $\text{m}^3 \text{m}^{-3}$), corresponding to pores more than 300 μm in diameter (Dexter and Czyz, 2007; Dexter et al., 2008), was calculated as:

$$\text{POR}_p = \text{POR}_t - \theta_{10} \quad (14)$$

where: $\text{POR}_t = (1 - \rho_t / \rho_p)$ is the total soil porosity calculated ($\text{m}^3 \text{m}^{-3}$) and θ_{10} the volumetric water content corresponding to the tension of a 10 cm water column ($\text{m}^3 \text{m}^{-3}$). Porosity in the domain of the soil matrix (POR_m , $\text{m}^3 \text{m}^{-3}$), corresponding to soil water content with pores less than 300 μm in diameter was estimated by using soil WRCs:

$$\text{POR}_m = \theta_{10} \quad (15)$$

Although there is no agreement in the literature about the best value for distinguishing macropores from matrix pores (Perret et al., 1999; Chen et al., 1993), we used the selected pore diameters due to the water and air storage characteristics which are very different. Thus, these pore sizes can be used for distinguishing different soil quality conditions (Reynolds et al., 2002).

Air Capacity and Air Capacity of Soil Matrix

Air capacity (AC_t , $\text{m}^3 \text{m}^{-3}$) was estimated from the total porosity calculated from θ_{100} ; the volumetric water content corresponding to the tension of a 100 cm water column.

$$\text{AC}_t = \text{POR}_t - \theta_{100} \quad (16)$$

Soil matrix air capacity was calculated by the equation:

$$AC_m = \theta_{10} - \theta_{100} \quad (17)$$

AC_m is the porosity corresponding to pores more than 30 μm and less than 300 μm in diameter.

Plant-available water capacity

For this purpose field capacity values (FC) were estimated, considering them as volumetric water content at a tension of 100 cm, and the permanent wilting point (PWP), was estimated as volumetric water content at a tension of 15,000 cm. Plant-available water capacity (PAWC) was estimated as: $PAWC = FC - PWP$ (Veihmeyer and Hendrickson, 1949). Finally the pore fraction with a diameter less (FC/POR_t) than and the pore fraction with a diameter more (AC_t/POR_t) than 30 μm were calculated as indicated by Reynolds et al. (2002).

The tension of 100 cm was used to define the field capacity water content due to pores with diameters < 30 μm and are considered as storage pores that contain water available for plants. In addition, these pores are influenced by texture and organic C content but not by increases in soil bulk density (da Silva and Kay, 1997; Kay and Angers, 2000).

Structural stability index

The risk of structural degradation was assessed by the "structural stability index" (SI) (Reynolds et al., 2009) calculated as:

$$SI = \frac{OM}{(\text{clay} + \text{silt})} \times 100 \quad (18)$$

where: OM is the organic matter content (g kg^{-1}); clay and silt are granulometric fractions (g kg^{-1}).

Global Index of soil physical quality

An index with a range between 0 and 1 was assigned to each attribute (OM, ρ_b , S_{gi} , AC_t , POR_p , PAWC, FC/POR_t and SI) according to the value obtained for each horizon. A value of 1 stands for the optimal condition for the attribute and 0 for the most limiting condition. As the value decreases, the condition becomes more unfavorable. The indexes between 1 and 0 were established taking into account the reference values mentioned in the literature for each parameter (Reynolds et al., 2009). Once all indexes were obtained, they were summed to produce the horizon score considering 8 as the maximum value, whereby eight attributes with an index of 1 each equals 100 %.

Five horizons with the highest score were used to draw an average WRC considered as an "average reference curve" for horizons with good structural quality. Additionally, the confidence interval for each normalized water content ($\Theta \pm \sigma$) was calculated, generating a curve

with minimal values and another with maximal values. For each one of these two curves d_{mean} , d_{mode} , d_{median} , SD, skewness and kurtosis parameters were determined, establishing a reference interval used to describe the shape of the curves and the pore frequency distribution of the horizons studied.

Relationships between indicators were studied using linear regression models in which the coefficient of determination (r^2) and statistical significance ($p < 0.05$) of the correlation were evaluated. In order to verify whether granulometric fractions, ρ_b and OM content affected S_{gi} values, a multiple regression analysis was carried out using a "stepwise" selection procedure (SAS, Statistical Analysis System, version 5.0, 1991). Analogously the relationship between structural quality index, SI, with ρ_b , POR_t , S_{gi} , POR_p , POR_m , AC_t , AC_m , FC, PWP, PAWC, FC/POR_t and AC_t/POR_t was analyzed.

Results and Discussion

Soil physical quality indicators

Only 14 A horizons showed values between 30 and 50 g kg^{-1} organic matter. All others presented lower values. Despite the wide particle size variation in the soils studied, an increase in ρ_b was observed when OM decreased (Figure 2).

Soil bulk density in A horizons was lower than the critical density estimated according to Daddow and Warrington (1983), even when various researches have demonstrated that small ρ_b increases can cause root growth reductions even if they are below the critical limit. Total porosity of the soil (POR_t) was between 0.432 and 0.567 $\text{m}^3 \text{m}^{-3}$. When analyzing air capacity (AC_t) corresponding to pores with diameters more than 30- μm diameter, the low values observed, especially in the B horizon, indicated evidence of the difficulties of these soils in terms of fluid flows. This indicator suggests the existence of reduced air volume to be used after heavy rainfall and confirms aeration problems found in different studies in the least limiting water range (Damiano and Moschini, 2011; Miretti et al., 2010).

Macroporosity (POR_p) was low. The POR_p geometric mean of all values in A horizon was 0.032 $\text{m}^3 \text{m}^{-3}$ and in B horizons 0.010 $\text{m}^3 \text{m}^{-3}$. Considering the optimal value of 0.07 $\text{m}^3 \text{m}^{-3}$ (Reynolds et al., 2009), in 42 cases, values were below this index and in 31, lower than 0.04 $\text{m}^3 \text{m}^{-3}$. Thus, in the soils studied the capacity to rapidly drain excess water and allow for root proliferation is not optimal due to the high content of silt or clay, the low sand content and the presence of occluded pores that are typical of the matrix in these soils (Taboada et al., 2008).

Physical quality degradation in these soils exacerbates these problems as evidenced in Argiudolls and Hapludolls irrigated with sodic-bicarbonated waters and in Argiudolls when conventional tillage or no-till systems were applied without the inclusion of adequate rotations (Pilatti et al., 2006; Ghiberto et al., 2007; Imhoff et al., 2010).

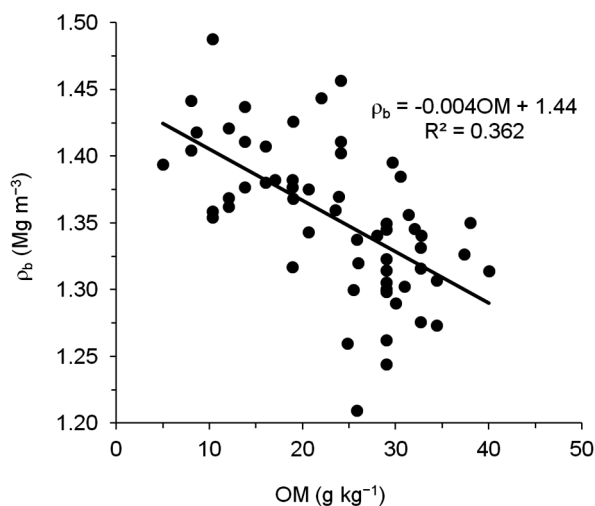


Figure 2 – Relationship between soil bulk density (ρ_b) and organic matter content (OM).

Small pore predominance was exhibited when evaluating the pore fraction of pores with less (FC/POR_t) and more (AC_t/POR_t) than 30- μ m diameters. Only in 13 cases, all in the A horizon, did FC/POR_t show values between 0.6 and 0.7. In 43 of all 60 cases this indicator was over 0.7 evidencing aeration and nitrate production problems due to the scarce amount of more than 30- μ m diameter pores present (Reynolds et al., 2002). The effect was noticeable in B horizons and both parameters presented a correlation with ρ_b as shown in Figure 3.

S_{gi} indicator variations ranged between 0.024 and 0.077 in A horizons and between 0.021 and 0.049 in B horizons (Table 2). Considering that the structural stability index $SI > 9$ % indicates a stable soil structure, $7\% < SI < 9\%$ a low degrading risk, $5\% < SI < 7\%$ a high degrading risk, $SI < 5\%$ structurally degraded soils (Reynolds et al., 2009), in 52 out of the 60 cases the value was $SI < 5\%$. This situation is a consequence of the high silt and clay content and the low organic matter proportion in the soils studied. On the other hand, SI was 10.8 when silt and clay content were 156 and 119 $g\ kg^{-1}$ respectively; this Hapludoll representing an extreme case among all soils analyzed because of its granulometry (sandy loam). Based on these considerations, the S_{gi} index was shown to be consistent with the results obtained, showing higher values with an increase in SI .

Taking into account the global index obtained for each horizon from OM, ρ_b , S_{gi} , AC_t , POR_p , PAWC, FC/POR_t and SI attributes, horizons could be organized into four groups presenting the following general characteristics.

Group 1 - With a score above 70 %, horizons show more than 15 % higher than 30 μ m (AC_t) diameter pores and macroporosity (POR_p) higher than 7 %. The FC/POR_t index is between 0.6 and 0.7, which ensures a proper balance between air and water supply. In these cases

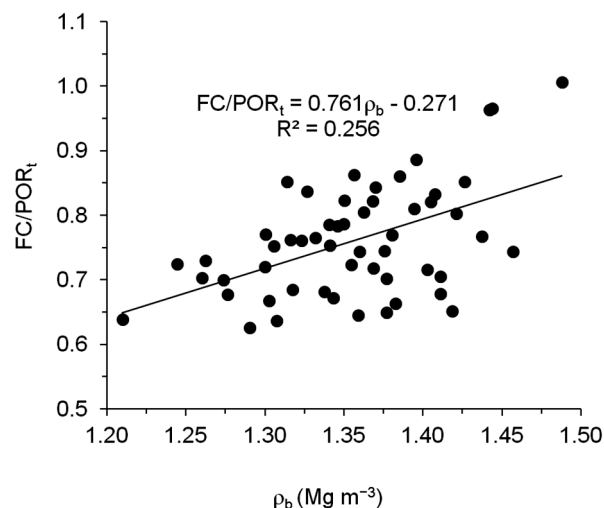


Figure 3 – Relationship between the fraction containing lower than 30 μ m diameter pores (FC/POR_t) and soil bulk density (ρ_b).

OM content ranged from adequate to optimal and was associated with good structural stability rates (SI). S_{gi} was between 0.035 and 0.05, indicating good physical quality. In soils with a high sand content and without a good capacity for water retention values were $S_{gi} > 0.05$.

Group 2 - Scoring between 50 and 70 %, AC_t continued at levels above 15 % but POR_p levels were lower than in the previous group, with values between 4 and 7 %. Horizons in this group appear to undergo structural degradation, a situation probably originated by the decrease in OM associated with the high silt content that is characteristic of the parent material of the Mollisols studied.

Group 3 - With a score below 50 %, their AC_t is lower than 15 % and their POR_p below 4 %, evidencing serious problems of air supply and water percolation.

Group 4 - B horizons have less than 10 % higher than 30 μ m diameter pores and less than 4 % higher than 300 μ m higher diameter pores, except for some horizons with over 15 % sand, the score being approximately 40 in these cases. For A horizons to surpass a score of 40 they should have approximately 3 % OM and lower than 1.3 $Mg\ m^{-3}$ ρ_b to compensate for the increased silt content in those horizons. Soils presenting B horizons with a score of about 40 (the highest one obtained in B horizons) would be the most productive ones and would be characterized by having a higher sand content and lower silt content than the rest, which seems to compensate for the lower OM content in A horizons of a similar score.

Water Retention Curves

Normalized water retention and pore distribution curves corresponding to A and B horizons of Mollisols

were studied together with the reference curve (Figure 4). The reference curve of A and B horizons was fitted to $\alpha = 0.053 \text{ cm}^{-1}$, $n = 1.1988$ and $m = 0.1658$ parameters, and was characterized by the values of d_{mode} that occurred at 72 % of saturation and a tension of $h = 84.5 \text{ cm}$, d_{median} that took place at 50 % saturation and $h = 609 \text{ cm}$, and d_{mean} with $h = 1,544 \text{ cm}$. As described by Blott and Pye

(2001) this distribution is "extremely poorly sorted" (i.e. very large range in equivalent pore diameters, $SD > 16$), "very fine skewed" (great excess of small equivalent pore diameters relative to a lognormal distribution, Skewness < -0.3), and "mildly leptokurtic" (slightly more peaked in the center and more tailed in the extremes than a lognormal distribution, Kurtosis = 1.11-1.50).

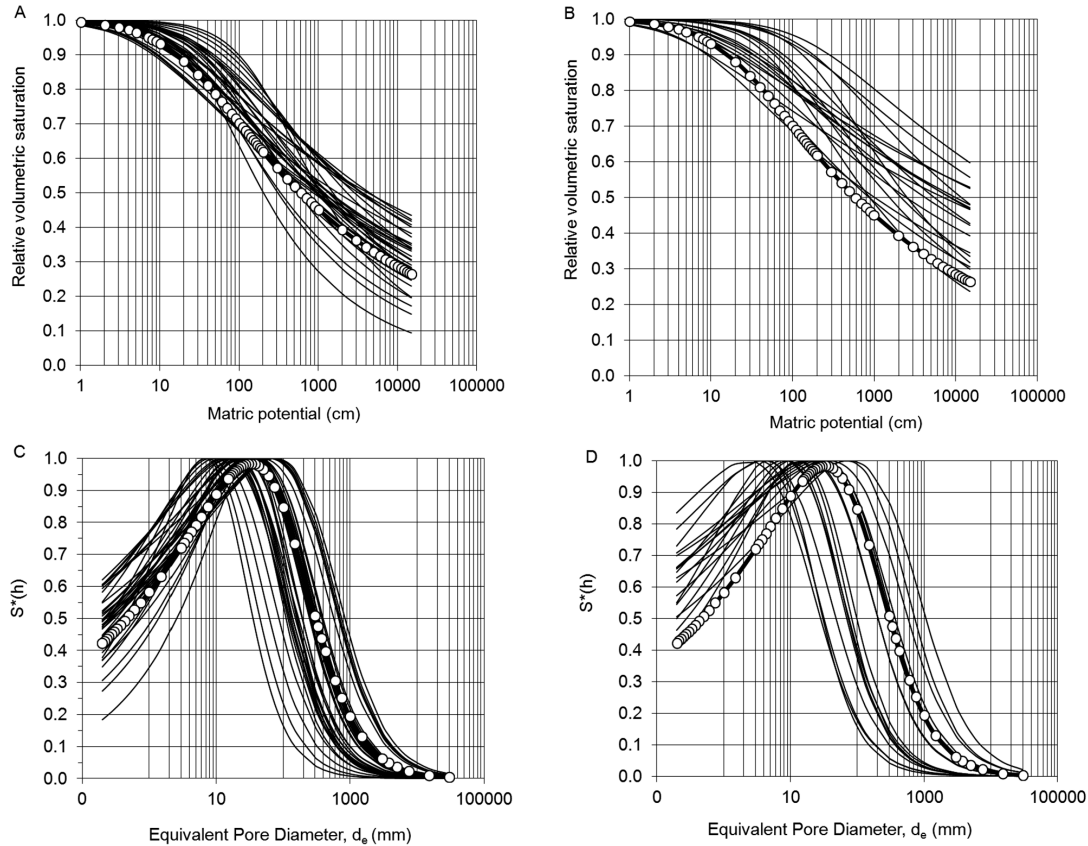


Figure 4 – Water retention curves and normalized pore frequency distribution curve (equation 2 and equation 5) corresponding to: (A) and (C) A horizons and (B) and (D) B horizons of the Mollisols studied. The reference curve is estimated from the five higher score horizons (black continuous dotted line).

Table 2 – Indicators of physical quality used to group the soils in categories.

		POR _p	AC _t	PAWC	FC/POR _t	SI	S _{gi}
		m ³ m ⁻³				%	-
A Horiz.	Mean	0.03	0.12	0.20	0.73	3.2	0.039
	Max.	0.09	0.19	0.31	0.89	10.8	0.077
	Min.	0.00	0.05	0.14	0.63	1.1	0.024
B Horiz.	Mean	0.01	0.06	0.18	0.83	1.5	0.030
	Max.	0.07	0.16	0.28	1.05	4.6	0.049
	Min.	0.00	0.02	0.12	0.65	0.5	0.021
Reference Values (†)		> 0.07(1)	> 0.15(1)	> 0.2(1)	0.6-0.7(1)	> 9.0(1)	> 0.05(1)
		0.07-0.04(0.5)	0.15-0.10(0.5)	0.15-0.2(0.7)		7.0-9.0(0.7)	0.035-0.05(0.7)
		< 0.04(0)	< 0.1(0)	0.1-0.15(0.3)	< 0.1(0)	7.0-5.0(0.3)	0.02-0.035(0.3)

POR_p: macroporosity; AC_t: air capacity; PAWC: plant-available water capacity; FC/POR_t: diameter pore fraction lower than 30 μm; SI: structural stability index; S_{gi}: S index. (†): Values between parentheses indicate the score assigned to the property in each horizon.

Table 3 – Measures of the central tendency, and parameters that describe the form of the curves and the pores' frequency distribution.

Parameter	d_{median}	d_{mode}	d_{mean}	SD	Skewness *	Kurtosis
	μm					
Group 1: Value >70	4.6	49.3	1.5	84.9	-0.40	1.14
Group 2: Value 50-70	3.7	32.4	1.3	118.9	-0.39	1.14
Group 3: Value < 50	2.2	21.2	0.8	73.5	-0.39	1.14
Group 4: B Horizons	0.5	14.1	0.1	103.1	-0.42	1.13
Reference Range [†]	3.4 – 6.8	31 – 39	1.2 – 3.0	68.7 – 145.4	-0.40 – -0.38	1.14 – 1.15

The values are the geometric means of the soils of each group, *arithmetic mean. [†]Calculated starting from the confidence interval of the reference curve($\theta \pm \sigma$), being the adjustment parameters for generating the minimum values $\alpha = 0.0545 \text{ cm}^{-1}$, $n = 1.2174$, $m = 0.1786$ and the maximum values $\alpha = 0.05143 \text{ cm}^{-1}$, $n = 1.18175$, $m = 0.1538$.

The values of skewness and kurtosis of the curves of the four soil groups were similar to the values of the reference curve (Table 3), but as physical quality becomes poorer, the characteristic pore diameter decreases. In particular, in Groups 3 and 4, central tendency measurements are outside the reference range indicating the existence of physical quality problems in these groups' horizons. These problems can also be inferred from Figure 4 where, especially for B horizons, in which for the same potential, soils present a higher effective saturation degree than in the reference curve. This is directly related to the higher amount of lower diameter pores and consequently, to aeration and drainage problems.

The reference curve can be also used to calculate effective saturation values at various matrix potentials (equation 2). Considering the average of five soils with higher scores of bulk density and particle density of 1.24 Mg m^{-3} and 2.55 Mg m^{-3} respectively, calculated POR_t would be $0.514 \text{ m}^3 \text{ m}^{-3}$. These were the values used to calculate POR_p . For this purpose the value of effective saturation was determined at $h = 10 \text{ cm}$ which, multiplied by total porosity, was equal to $0.035 \text{ m}^3 \text{ m}^{-3}$. Similarly, AC_t was determined, being $0.153 \text{ m}^3 \text{ m}^{-3}$, FC $0.361 \text{ m}^3 \text{ m}^{-3}$, PWP $0.136 \text{ m}^3 \text{ m}^{-3}$ and PAWC $0.225 \text{ m}^3 \text{ m}^{-3}$. The pore fraction, having a pore diameters lower (FC/POR_t) than $30 \text{ }\mu\text{m}$, would be 0.7 and the one higher (AC_t/POR_t) than $30\text{-}\mu\text{m}$ diameter would be 0.3. These values are within the range mentioned by other authors (Orellana and Pilatti, 2000; Pilatti et al., 2012; Reynolds et al., 2002; Reynolds et al., 2009) and represent useful indicators for guiding sustainable soil management.

Conclusion

Porosity in the macropore domain was low. A small decrease can, in this domain, cause severe physical restrictions in soils with a high silt percentage. Then, the capacity to rapidly drain water excesses and allow for root proliferation is not optimal due to the high silt or clay content, in A and B horizons respectively, and the low sand content which are characteristic of the matrix of the soils studied.

References

- Blake, G.R.; Hartge, K.H. 1986a. Particle density. p. 377-382. In: Klute, A., ed. Methods of soil analysis. Part I. Physical and mineralogical methods. 2ed. ASA/SSSA, Madison, MI, USA.
- Blake, G.R.; Hartge, K.H. 1986b. Bulk density. p. 363-375. In: Klute, A., ed. Methods of soil analysis. Part I. Physical and mineralogical methods. 2ed. ASA/SSSA, Madison, MI, USA.
- Blott, S.J.; Pye, K. 2001. Gradistat: a grain size distribution and statistics package for the analysis of unconsolidated sediments. *Earth Surface Processes and Landforms* 26: 1237-1248.
- Bronick, C.J.; Lal, R. 2005. Soil structure and management: a review. *Geoderma* 124: 3-22.
- Chen, C.; Thomas, D.M.; Green, R.E.; Wagenet, R.J. 1993. Two-domain estimation of hydraulic properties in macropore soils. *Soil Science Society of America Journal* 57: 680-686.
- Clothier, B.E.; Green, S.R.; Deurer, M. 2008. Preferential flow and transport in soil: progress and prognosis. *European Journal of Soil Science* 59: 2-13.
- Daddow, R.L.; Warrington, G.E. 1983. Growth-limiting soil bulk densities as influenced by soil texture. USDA Forest Service, Fort Collins, CO, USA. (WSDG Report. WSDG-TN-00005).
- Damiano, F.; Moschini, R.C. 2011. Least limiting water range in Argiudoll soils under Eucalyptus dunnii maiden. *Ciencia del Suelo* 29: 1-11 (in Spanish, with abstract in English).
- Dexter, A.R.; Czyz, E.A.; Richard, G.; Reszkowska, A. 2008. A user friendly water retention function that takes account of the textural and structural pore space in soil. *Geoderma* 143: 243-253.
- Dexter, A.R.; Czyz, E.A. 2007. Applications of S-theory in the study of soil physical degradation and its consequences. *Land Degradation and Development* 18: 369-381.
- Dexter, A.R. 2004a. Soil physical quality. Part I. Theory, effects of soil texture, density, and organic matter, and effects on root growth. *Geoderma* 120: 201-214.
- Dexter, A.R. 2004b. Soil physical quality. Part II. Friability, tillage, tilling and hard-setting. *Geoderma* 120: 215-225.
- Dexter, A.R. 2004c. Soil physical quality. Part III: Unsaturated hydraulic conductivity and general conclusions about S-Theory. *Geoderma* 120: 227-239.
- Gee, G.W.; Bauder, J.C. 1986. Particle size analysis. p. 383-411. In: Klute, A., ed. Methods of soil analysis. Part I. Physical and mineralogical methods. 2ed. ASA/SSSA, Madison, MI, USA.

- Genuchten, M.T. van. 1980. A closed-form equation for predicting the hydraulic conductivity of unsaturated soils. *Soil Science Society of America Journal* 44: 892-898.
- Genuchten, M.T. van; Simunek, J.; Leij, F.J.; Sejna, M. 2007. Code for quantifying the hydraulic functions of unsaturated soils – RETC Version 6.0. US Salinity Laboratory, Riverside. Available at: <http://www.pc-progress.com/en/Default.aspx> [Accessed Sep 5, 2011]
- Ghiberto, P.J.; Pilatti, M.; Imhoff, S.; Orellana, J.A. 2007. Hydraulic conductivity of Molisolls irrigated with sodic-bicarbonated waters in Santa Fe (Argentina). *Agricultural Water Management* 88: 192-200.
- Imhoff, S.; Ghiberto, P.J.; Grioni, A.; Gay, J.P. 2010. Porosity characterization of Argiudolls under different management systems in the flat Pampas of Argentina. *Geoderma* 158: 268-274.
- Instituto Nacional de Tecnología Agropecuaria [INTA] 2014. GeoINTA viewer: soil maps, soil profiles and soil coverage, images and georeferenced databases = Visor GeoINTA: mapas de suelo, perfiles y coberturas de suelos, imágenes y bases de datos georeferenciadas. Available at: <http://geointa.inta.gov.ar/visor2/?p=96> [Accessed Jul 11, 2014] (in Spanish).
- Jackson, M.L. 1982. *Soil Chemical Analysis. = Análisis Químico de Suelos*. Omega, Barcelona, Spain (in Spanish).
- Kay, B.D.; Angers, D.A. 2000. Soil structure. p. A229-A276. In: Sumner, M.E., ed. *Handbook of soil science*. CRC Press, Boca Raton, FL, USA.
- Klute, A. 1986. Water retention: laboratory methods. p. 635-660. In: Klute, A., ed. *Methods of soil analysis. Part I. Physical and mineralogical methods*. 2ed. ASA/ SSSA, Madison, MI, USA.
- Libardi, P.L. 2005. *Dynamics of Soil Water = Dinâmica da Água no Solo*. EDUSP, São Paulo, SP, Brazil (in Portuguese).
- Miretti, M.C.; Imhoff, S.; Silva, A.P.; Lavado, R. 2010. Soil structure degradation in patches of alfalfa fields. *Scientia Agricola* 67: 604-610.
- Orellana, J.A. de; Pilatti, M.A. 2000. The ideal soil: II. Critical values of an "ideal soil", for Mollisols in the north of the Pampean region (in Argentina). *Journal of Sustainable Agriculture* 17: 89-109.
- Perret, J.; Prasher, S.O.; Kantzas, A.; Langford, C. 1999. Three-dimensional quantification of macropore networks in undisturbed soil cores. *Soil Science Society of America Journal* 63: 1530-1543.
- Pilatti, M.A.; Orellana, J.A.; Imhoff, S.C.; Silva, A.P. 2012. Review of the critical limits of the optimal hydric interval. *Ciencia del Suelo* 30: 9-21 (in Spanish, with abstract in English).
- Pilatti, M.A.; Imhoff, S.; Ghiberto, P.J.; Marano, R.P. 2006. Changes in some physical properties of Mollisols induced by supplemental irrigation. *Geoderma* 133: 431-443.
- Reynolds, W.D.; Drury, C.F.; Tan, C.S.; Fox, C.A.; Yang, X.M. 2009. Use of indicators and pore volume-function characteristics to quantify soil physical quality. *Geoderma* 152: 252-263.
- Reynolds, W.D.; Bowman, B.T.; Drury, C.F.; Tan, C.S. 2002. Indicators of good soil physical quality: density and storage parameters. *Geoderma* 110: 131-146.
- Silva, A.P.; Kay, B.D. 1997. Effect of soil water content variation on the least limiting water range. *Soil Science Society of America Journal* 61: 877-883.
- Taboada, M.A.; Barbosa, O.A.; Cosentino, D.J. 2008. Null creation of air-filled structural pores by soil cracking and shrinkage in silty loamy soils. *Soil Science* 173: 130-142.
- Veihmeyer, F.J.; Hendrickson, A.H. 1949. Methods of measuring field capacity and permanent wilting percentage of soils. *Soil Science* 68: 75-94.